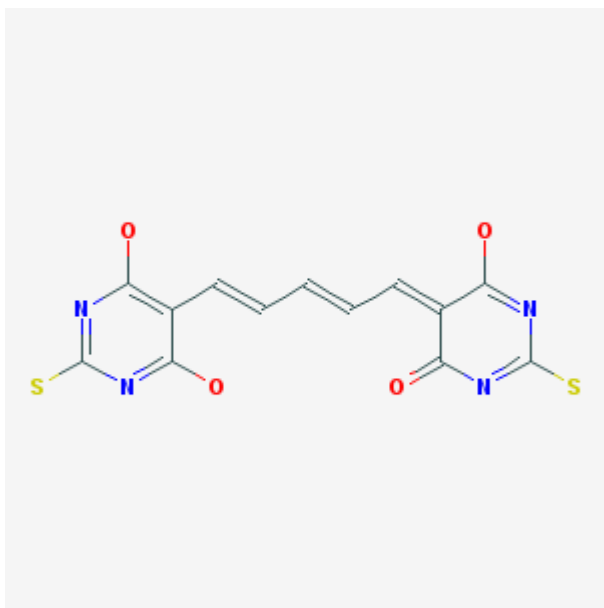


# 5-(2E,4E)-5-(6-hydroxy-4-oxo-2-thioxo-1,2,3,4-tetrahydro-5 pyrimidinyl)-2,4-pentadienylidene-2-thioxodihydro-4,6(1H,5H)-pyrimidinedione

THK-265

Kam Leung, PhD<sup>1</sup>

Created: July 1, 2012; Updated: October 25, 2012.

<b>Chemical name:</b>	5-(2E,4E)-5-(6-hydroxy-4-oxo-2-thioxo-1,2,3,4-tetrahydro-5 pyrimidinyl)-2,4-pentadienylidene-2-thioxodihydro-4,6(1H,5H)-pyrimidinedione	
<b>Abbreviated name:</b>	THK-265	
<b>Synonym:</b>		
<b>Agent category:</b>	Compound	
<b>Target:</b>	Amyloid-beta (Aβ) peptide	
<b>Target category:</b>	Acceptor	
<b>Method of detection:</b>	Optical, near-infrared (NIR) fluorescence imaging	
<b>Source of signal:</b>	THK-265	
<b>Activation:</b>	No	

*Table continues on next page...*

<sup>1</sup> National Center for Biotechnology Information, NLM, NIH, Bethesda, MD; Email: micad@ncbi.nlm.nih.gov.

✉ Corresponding author.

Table continued from previous page.

<b>Studies:</b>	<ul style="list-style-type: none"> <li>• <i>In vitro</i></li> <li>• Rodents</li> </ul>	Click on the above structure for additional information in <a href="#">PubChem</a> .
-----------------	--	--

## Background

[[PubMed](#)]

Alzheimer's disease (AD) is a form of dementia with gradual memory loss and a progressive decline in mental functions over time (1, 2). It is characterized pathologically by neuronal loss, extracellular senile plaques (aggregates of amyloid-beta ( $A\beta$ ) peptides consisting of 40–42 amino acids formed as the proteolytic cleavage of  $A\beta$  protein precursor ( $A\beta$ PP)), and intracellular neurofibrillary tangles (filaments of microtubule-binding hyper-phosphorylated protein tau) in the brain, especially in the hippocampus and associative regions of the cortex (3, 4).  $A\beta$  peptides and tau protein are implicated as the main causes of neuronal degeneration and cell death (5, 6). Early diagnosis of AD is important for treatment consideration and disease management (7). Various  $A\beta$  imaging agents have been developed for magnetic resonance imaging (MRI), single-photon emission computed tomography (SPECT), and positron emission tomography (PET) (8–13). The binding of different derivatives of Congo red, thioflavin, stilbene, and aminonaphthalene has been studied in human postmortem brain tissue and in transgenic mice. 2-(1-(6-[(2- $^{18}\text{F}$ fluoroethyl)(methyl)amino]-2-naphthyl)ethylidene)malono nitrile ( $^{18}\text{F}$ FDDNP) has been studied in humans, showing more binding in the brains of patients with AD than in those of healthy people (14). However,  $^{18}\text{F}$ FDDNP showed low signal/noise ratios for PET imaging because it is highly lipophilic. *N*-methyl- $^{11}\text{C}$ -2-(4'-methylaminophenyl)-6-hydroxybenzothiasole, a  $A\beta$  binding compound based on a series of neutral thioflavin-T derivatives (15), was radiolabeled with the positron-emitting radionuclide  $^{11}\text{C}$  ( $^{11}\text{C}$ 6-OH-BTA-1 or  $^{11}\text{C}$ PIB).  $^{11}\text{C}$ 6-OH-BTA-1 was found to be a promising imaging agent for senile plaques in the brain (16). Zhang et al. (17) reported the development of a series of fluorinated polyethylene glycol (PEG) units ( $n = 2-5$ ) for PET imaging of  $A\beta$  plaques in the brain. Two of them,  $^{18}\text{F}$ BAY94-9172 ( $^{18}\text{F}$ AV-1) (18) and ( $^{18}\text{F}$ AV-45, also known as  $^{18}\text{F}$ Florbetapir) (19), have been evaluated in clinical trials.  $^{18}\text{F}$ Florbetapir is approved for estimation of brain amyloid plaque content in patients with cognitive decline by the United States Food and Drug Administration ([US FDA](#)).

NLM Citation: Leung K. 5-(2*E*,4*E*)-5-(6-hydroxy-4-oxo-2-thioxo-1,2,3,4-tetrahydroxy-5-pyrimidinyl)-2,4-pentadienylidene-2-thioxodihydro-4,6(1*H*,5*H*)-pyrimidinedione. 2012 Jul 1 [Updated 2012 Oct 25]. In: Molecular Imaging and Contrast Agent Database (MICAD) [Internet]. Bethesda (MD): National Center for Biotechnology Information (US); 2004-2013.

Optical imaging is increasingly being used to monitor biological functions of specific targets *in vitro* and *in vivo* to provide real-time imaging (20-22). Small near-infrared (NIR) fluorescence probes (emission wavelength, 650–900 nm) exhibit a reduction of the natural background fluorescence interference of biomolecules, providing a high contrast between target and background tissues in small animals. A number of optical probes for the detection of A $\beta$  plaques are available, such as Congo red, thioflavin, CRANAD-2, and AOI987 (23, 24). Okamura et al. (25) evaluated 5-(2*E*,4*E*)-5-(6-hydroxy-4-oxo-2-thioxo-1,2,3,4-tetrahydroxy-5 pyrimidinyl)-2,4-pentadienyliidene-2-thioxodihydro-4,6(1*H*,5*H*)-pyrimidinedione (THK-265) as a NIR fluorescence imaging probe for *in vivo* imaging of A $\beta$  in an animal model of AD.

### Related Resource Links:

- Chapters in MICAD ([amyloid](#))
- Gene information in NCBI ([amyloid](#))
- Articles in Online Mendelian Inheritance in Man (OMIM) ([amyloid](#))
- Clinical trials ([amyloid](#))
- Drug information in FDA ([amyloid inhibitors](#))

## Synthesis

[PubMed]

THK-265 is commercially available (Organica, Wolfen, Germany) (25). THK-265 displayed the following fluorescent properties in methanol: one single absorption maximum at 627 nm, one single emission maximum at 644 nm, a high absorption coefficient of  $96,198 \text{ M}^{-1}\text{cm}^{-1}$ , and a high quantum yield of 38.5%. Similar maximum excitation and emission wavelengths were observed in human serum and potassium phosphate buffer (pH, 7.4). THK-265 exhibited a log *P* value of  $1.8 \pm 0.8$  (moderate lipophilicity).

## *In Vitro* Studies: Testing in Cells and Tissues

[PubMed]

Differential fluorescence spectroscopy performed by Okamura et al. (25) showed that the magnitude of the fluorescence increase was dependent on the concentration of THK-265 (3–1,000 nM) in the presence of aggregated A $\beta$  peptides (5  $\mu\text{M}$ ). The  $K_d$  value for THK-265 was estimated to be  $97 \pm 5 \text{ nM}$ , which was lower than that of AOI987 (200 nM). THK-265 staining of amyloid plaques was observed in postmortem brain tissues of the brain (the surface region of frontal cortex) of one AD male patient (age 69 years). THK-265 staining pattern colocalized with A $\beta$  immunostaining. THK-265 also stained neurofibrillary tangles.

## Animal Studies

### Rodents

[PubMed]

The blood–brain barrier (BBB) penetration of THK-265 was assessed *ex vivo* using 7-week-old wild-type (Wt) male mice ( $n = 3\text{--}4/\text{group}$ ) after intravenous injection of 1 mg/kg THK-265 (25). Brain accumulation levels of THK-265 were 0.04% injected dose per gram (ID/g) at 2 min and 0.0065% ID/g at 30 min as measured with high-performance liquid chromatography. *Ex vivo* NIR fluorescence imaging showed that THK-265 entered the brain rapidly ( $6.2 \times 10^7$  p/s/cm<sup>2</sup>/sr) at 2 min and was then gradually eliminated from the brain, with  $2.4 \times 10^7$  p/s/cm<sup>2</sup>/sr and  $2.1 \times 10^7$  p/s/cm<sup>2</sup>/sr at 60 min and 120 min, respectively. No acute toxicity of THK-265 at 10 mg/kg in normal mice was observed up to 7 days after injection.

*In vivo* NIR fluorescence imaging of A $\beta$  using THK-265 (1 mg/kg) was performed in 19-month-old (19M) and 32-month-old (32M) A $\beta$ PP transgenic (Tg) and age-matched Wt female mice ( $n = 3/\text{group}$ ) at 0, 3, 30, 64, and 118 min after injection (25). THK-265 entered rapidly into the brains and was consistently higher in Tg mice than in Wt mice. Fluorescence intensity levels at 3 min after injection were 3.8, 2.6, 1.8, and  $1.7 \times 10^8$  p/s/cm<sup>2</sup>/sr for 32M Tg, 19M Tg, 32M Wt, and 19M Wt mice, respectively. Additional studies were performed in 27M Tg and 27M Wt mice with THK-265, AOI987, and ICG. Both THK-265 and AOI987 showed higher fluorescence signals in Tg mice than in Wt mice, whereas ICG showed similar fluorescence signals in both types of mice. The brain/neck ratios at 113 min after injection were 1.2, 1.2, 1.2, 1.6, 1.3, and 2.2 for ICG/Wt, ICG/Tg, AOI987/Wt, AOI987/Tg, THK-265/Wt, and THK-265/Tg, respectively. THK-265 displayed similar brain/neck ratios with AOI987 and ICG in the Wt mice but significantly higher ratios than AOI987 and ICG in the Tg mice ( $P < 0.05$ ). There was a significant correlation ( $r = 0.943$ ,  $P < 0.017$ ) of THK-265 brain/neck ratios with the number of amyloid plaques in Tg mice.

Schmidt et al. (26) performed *in vivo* NIR fluorescence imaging of A $\beta$  using THK-265 (1 mg/kg) using younger Tg and Wt mice (75, 100, and 200 d) ( $n = 5/\text{group}$ ) at 10, 20, 30, 60, and 90 min after injection. There was an increase of signal in the Tg mice correlating with age, whereas little change in signal was observed in Wt mice *versus* baseline background. Quantitative analysis of fluorescence signals in the brain at 30 min after injection showed that Tg (75 d), Tg (100 d), and Tg (200 d) mice exhibited 20%, 80%, and 140% increase in signal compared with the age-matched Wt mice. Histological analysis showed that there was co-localization of THK-265 staining with amyloid plaques and an increasing number of amyloid plaques with stronger fluorescence signal.

### Other Non-Primate Mammals

[PubMed]

No publication is currently available.

## Non-Human Primates

[PubMed]

No publication is currently available.

## Human Studies

[PubMed]

No publication is currently available.

## References

1. Forstl H., Kurz A. *Clinical features of Alzheimer's disease*. Eur Arch Psychiatry Clin Neurosci. 1999;249(6):288–90. PubMed PMID: 10653284.
2. Heininger K. *A unifying hypothesis of Alzheimer's disease. IV. Causation and sequence of events*. Rev Neurosci. 2000;11(Spec No):213–328. PubMed PMID: 11065271.
3. Mirra S.S., Heyman A., McKeel D., Sumi S.M., Crain B.J., Brownlee L.M., Vogel F.S., Hughes J.P., van Belle G., Berg L. *The Consortium to Establish a Registry for Alzheimer's Disease (CERAD). Part II. Standardization of the neuropathologic assessment of Alzheimer's disease*. Neurology. 1991;41(4):479–86. PubMed PMID: 2011243.
4. Hardy J.A., Higgins G.A. *Alzheimer's disease: the amyloid cascade hypothesis*. Science. 1992;256(5054):184–5. PubMed PMID: 1566067.
5. Hardy J. *The relationship between amyloid and tau*. J Mol Neurosci. 2003;20(2):203–6. PubMed PMID: 12794314.
6. Brandt R., Hundelt M., Shahani N. *Tau alteration and neuronal degeneration in tauopathies: mechanisms and models*. Biochim Biophys Acta. 2005;1739(2-3):331–54. PubMed PMID: 15615650.
7. de Leon M.J., DeSanti S., Zinkowski R., Mehta P.D., Pratico D., Segal S., Clark C., Kerkman D., DeBernardis J., Li J., Lair L., Reisberg B., Tsui W., Rusinek H. *MRI and CSF studies in the early diagnosis of Alzheimer's disease*. J Intern Med. 2004;256(3):205–23. PubMed PMID: 15324364.
8. Bacskai B.J., Klunk W.E., Mathis C.A., Hyman B.T. *Imaging amyloid-beta deposits in vivo*. J Cereb Blood Flow Metab. 2002;22(9):1035–41. PubMed PMID: 12218409.
9. Nordberg A. *PET imaging of amyloid in Alzheimer's disease*. Lancet Neurol. 2004;3(9):519–27. PubMed PMID: 15324720.
10. Mathis C.A., Wang Y., Klunk W.E. *Imaging beta-amyloid plaques and neurofibrillary tangles in the aging human brain*. Curr Pharm Des. 2004;10(13):1469–92. PubMed PMID: 15134570.
11. Klunk W.E., Engler H., Nordberg A., Bacskai B.J., Wang Y., Price J.C., Bergstrom M., Hyman B.T., Langstrom B., Mathis C.A. *Imaging the pathology of Alzheimer's disease:*

- amyloid-imaging with positron emission tomography*. Neuroimaging Clin N Am. 2003;13(4):781–9. PubMed PMID: 15024961.
12. Wang Y., Klunk W.E., Debnath M.L., Huang G.F., Holt D.P., Shao L., Mathis C.A. *Development of a PET/SPECT agent for amyloid imaging in Alzheimer's disease*. J Mol Neurosci. 2004;24(1):55–62. PubMed PMID: 15314250.
  13. Kung M.P., Hou C., Zhuang Z.P., Skovronsky D., Kung H.F. *Binding of two potential imaging agents targeting amyloid plaques in postmortem brain tissues of patients with Alzheimer's disease*. Brain Res. 2004;1025(1-2):98–105. PubMed PMID: 15464749.
  14. Shoghi-Jadid K., Small G.W., Agdeppa E.D., Kepe V., Ercoli L.M., Siddarth P., Read S., Satyamurthy N., Petric A., Huang S.C., Barrio J.R. *Localization of neurofibrillary tangles and beta-amyloid plaques in the brains of living patients with Alzheimer disease*. Am J Geriatr Psychiatry. 2002;10(1):24–35. PubMed PMID: 11790632.
  15. Bacskai B.J., Hickey G.A., Skoch J., Kajdasz S.T., Wang Y., Huang G.F., Mathis C.A., Klunk W.E., Hyman B.T. *Four-dimensional multiphoton imaging of brain entry, amyloid binding, and clearance of an amyloid-beta ligand in transgenic mice*. Proc Natl Acad Sci U S A. 2003;100(21):12462–7. PubMed PMID: 14517353.
  16. Klunk W.E., Engler H., Nordberg A., Wang Y., Blomqvist G., Holt D.P., Bergstrom M., Savitcheva I., Huang G.F., Estrada S., Ausen B., Debnath M.L., Barletta J., Price J.C., Sandell J., Lopresti B.J., Wall A., Koivisto P., Antoni G., Mathis C.A., Langstrom B. *Imaging brain amyloid in Alzheimer's disease with Pittsburgh Compound-B*. Ann Neurol. 2004;55(3):306–19. PubMed PMID: 14991808.
  17. Zhang W., Oya S., Kung M.P., Hou C., Maier D.L., Kung H.F. *F-18 Polyethyleneglycol stilbenes as PET imaging agents targeting Abeta aggregates in the brain*. Nucl Med Biol. 2005;32(8):799–809. PubMed PMID: 16253804.
  18. O'Keefe G.J., Saunder T.H., Ng S., Ackerman U., Tochon-Danguy H.J., Chan J.G., Gong S., Dyrks T., Lindemann S., Holl G., Dinkelborg L., Villemagne V., Rowe C.C. *Radiation Dosimetry of {beta}-Amyloid Tracers 11C-PiB and 18F-BAY94-9172*. J Nucl Med. 2009;50(2):309–15. PubMed PMID: 19164222.
  19. Choi S.R., Golding G., Zhuang Z., Zhang W., Lim N., Hefti F., Benedum T.E., Kilbourn M.R., Skovronsky D., Kung H.F. *Preclinical properties of 18F-AV-45: a PET agent for Abeta plaques in the brain*. J Nucl Med. 2009;50(11):1887–94. PubMed PMID: 19837759.
  20. Frangioni J.V. *New technologies for human cancer imaging*. J Clin Oncol. 2008;26(24):4012–21. PubMed PMID: 18711192.
  21. Pan D., Caruthers S.D., Chen J., Winter P.M., SenPan A., Schmieder A.H., Wickline S.A., Lanza G.M. *Nanomedicine strategies for molecular targets with MRI and optical imaging*. Future Med Chem. 2010;2(3):471–90. PubMed PMID: 20485473.
  22. Schaafsma B.E., Mieog J.S., Hutteman M., van der Vorst J.R., Kuppen P.J., Lowik C.W., Frangioni J.V., van de Velde C.J., Vahrmeijer A.L. *The clinical use of indocyanine green as a near-infrared fluorescent contrast agent for image-guided oncologic surgery*. J Surg Oncol. 2011;104(3):323–32. PubMed PMID: 21495033.
  23. Hintersteiner M., Enz A., Frey P., Jatton A.L., Kinzy W., Kneuer R., Neumann U., Rudin M., Staufenbiel M., Stoekli M., Wiederhold K.H., Gremlich H.U. *In vivo detection of amyloid-beta deposits by near-infrared imaging using an oxazine-derivative probe*. Nat Biotechnol. 2005;23(5):577–83. PubMed PMID: 15834405.

24. Ran C., Xu X., Raymond S.B., Ferrara B.J., Neal K., Bacskai B.J., Medarova Z., Moore A. *Design, synthesis, and testing of difluoroboron-derivatized curcumins as near-infrared probes for in vivo detection of amyloid-beta deposits.* J Am Chem Soc. 2009;131(42):15257–61. PubMed PMID: 19807070.
25. Okamura N., Mori M., Furumoto S., Yoshikawa T., Harada R., Ito S., Fujikawa Y., Arai H., Yanai K., Kudo Y. *In vivo detection of amyloid plaques in the mouse brain using the near-infrared fluorescence probe THK-265.* J Alzheimers Dis. 2011;23(1):37–48. PubMed PMID: 20930313.
26. Schmidt A., Pahnke J. *Efficient Near-Infrared In Vivo Imaging of Amyloid-beta Deposits in Alzheimer's Disease Mouse Models.* J Alzheimers Dis. 2012;30(3):651–64. PubMed PMID: 22460331.